Necessary Conditions for the Emergence of Homochirality *via* Autocatalytic Self-replication

Michael Stich,[1] Josep M. Ribó,[2] Donna G. Blackmond,[3,*] and David Hochberg[4,†]

[1] *Non-linearity and Complexity Research Group, System Analytics Research Institute, School of Engineering and Applied Science, Aston University, B4 7ET Birmingham, UK*

[2] *Department of Organic Chemistry, Institute of Cosmos Science (IEEC-UB), University of Barcelona, Barcelona, Spain*

[3] *Department of Chemistry, The Scripps Research Institute, La Jolla, CA 93207 USA*

[4] *Department of Molecular Evolution, Centro de Astrobiología (CSIC-INTA), Carretera Ajalvir Kilómetro 4, 28850 Torrejón de Ardoz, Madrid, Spain*

(Dated: June 30, 2016)

Abstract

We analyze a recent proposal for spontaneous mirror symmetry breaking based on the coupling of first-order enantioselective autocatalysis and direct production of the enantiomers that invokes a critical role for intrinsic reaction noise. For isolated systems, the racemic state is the unique stable outcome for both stochastic and deterministic dynamics when the system is in compliance with the constraints dictated by the thermodynamics of chemical reaction processes. In open systems, the racemic outcome also results for both stochastic and deterministic dynamics when driving the autocatalysis unidirectionally by external reagents. Nonracemic states can result in the latter only if the reverse reactions are strictly zero: these are kinetically controlled outcomes for small populations and volumes, and can be simulated by stochastic dynamics. However, the stability of the thermodynamic limit proves that the racemic outcome is the unique stable state for strictly irreversible externally driven autocatalysis. These findings contradict the suggestion that the inhibition requirement of the Frank autocatalytic model for the emergence of homochirality may be relaxed in a noise-induced mechanism.

PACS numbers: 05.40.Ca, 11.30.Qc, 87.15.B-

* blackmond@scripps.edu

† hochbergd@cab.inta-csic.es

I. INTRODUCTION

The observed bias in biopolymers composed from homochiral L-amino acids and D-sugars is a remarkable feature of biological chemistry. There is a general consensus that the homochirality of biological compounds is a condition associated to life that probably emerged through processes of spontaneous mirror symmetry breaking (SMSB) [1]. SMSB involves transformations yielding nonracemic outcomes as non-equilibrium steady states (NESS), and in the absence of any chiral polarization or external chiral physical forces [2–6]. Homochirality could have emerged following symmetry breaking by incorporating steps of increasing complexity leading to chemical systems and enantioselective chemical networks [7, 8]. In a classic paper published in 1953, Frank [9] postulated that a molecule able to replicate itself while suppressing replication of its mirror image (enantiomer) provides "a simple and sufficient life model" for the emergence of homochirality from a stochastically racemic mixture of enantiomers. This deceptively simple mathematical model of self-replication and mirror-image inhibition spurred decades of research seeking an experimental proof of concept, ultimately demonstrated by Soai and coworkers in 1995 [10]. To date, the Soai reaction (see scheme in Fig 1) remains the only documented experimental example of autocatalytic enantioenrichment, and the system has served as a model for how homochirality might emerge [11]. Because these particular chemical transformations would not occur under prebiotically relevant conditions, however, the Soai reaction itself does not provide a definitive explanation linked to the origin of life. While theoretical work continues to provide interesting new perspectives by expanding and modifying the Frank autocatalytic model, the experimental search for a prebiotically plausible autocatalytic reaction system that amplifies enantiomeric excess has become something of a "Holy Grail" in the Origin of Life research community.

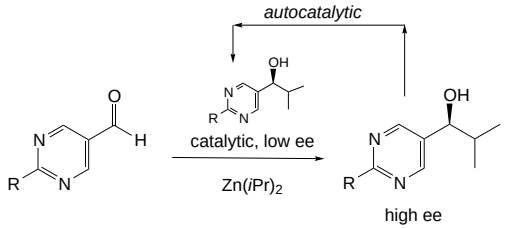

FIG. 1. Soai Autocatalytic Reaction: Amplification of Product Enantiomeric Excess

If ongoing theoretical research is to be of practical aid in this experimental search, it is

important that such studies be well-grounded in the basic principles that dictate the chemical and physical behavior of molecules. This point has been discussed most frequently in the context of principles of chemical thermodynamics governing the reversibility of reactions [12, 13]. Most recently, a modeling study by Goldenfeld and coworkers [14] developed an extension of the Frank model aiming to show that the original model's inhibition criterion is unnecessary. They reported that in a non-equilibrium steady-state system, homochirality may emerge from the racemic state by a noise-induced mechanism. The purpose of the present work is to provide a critical analysis of that work to determine if the computationally imposed reactivity is consistent with the fundamental chemical laws constraining the system. An assessment of the conclusions of that model follows this analysis, along with a discussion of the outlook for experimental systems.

II. BACKGROUND

Theoretical proposals for the emergence of homochirality in abiotic chemical evolution are based either on deterministic or on chance events, which may involve chemical reactions or physical rate processes [1, 2, 15]. Reaction rate equations are customarily employed to cast chemical reaction schemes in terms of coupled differential equations for the evolution of the concentrations of the species involved. In this deterministic approach, initial conditions must be taken to simulate the inherent statistical fluctuations about the ideal racemic composition [16, 17]. In contrast, chemical reactions are inherently stochastic in nature: the reagents in solution (or attached on surfaces) must encounter each other before they can react, and the probability per unit time for the reaction to occur is related to the corresponding reaction rate constant. The discrete molecular nature of chemical reagents and reactions gives rise to the concept of intrinsic reaction noise [18]. Despite the fact that stochastic and deterministic kinetics must coincide in the thermodynamic limit (i.e., for large numbers of molecules and large volumes while keeping the species concentrations constant), stochastic methods can be used to explore the issue of whether noise affects the final outcome of the underlying reaction, for finite size systems and small populations of molecules.

Stochastic methods are necessary to describe kinetic dynamics in the case of small volumes and/or small numbers of reacting molecules [19, 20], as is the case, for example, in compartmentalized cellular processes [21]. Therefore, the differences, if any, in the evolution

of the enantiomeric excess (ee) between deterministic and stochastic kinetics could provide insights regarding asymmetric inductions and SMSB processes in prebiotic models. In this respect, Goldenfeld and coworkers recently reported that reaction noise in a closed model involving strictly irreversible enantioselective autocatalysis coupled with the uncatalyzed, reversible production of the enantiomers stabilizes the homochiral states, making these the most probable outcome of the system [14].

The purpose of this paper is to analyze in more detail the role of reaction noise in asymmetric autocatalytic reaction networks in the context of this proposal. In Sec III we discuss the kinetic model of Ref. [14] in the context of basic principles of chemical kinetics and thermodynamics. In Sec IV we consider for well-mixed systems the influence that reaction noise has on the stationary states of the scheme proposed in Ref. [14], once the dictates of chemical thermodynamics are correctly accounted for. In Sec V we address the coupling of the autocatalytic reactions to external chemical energy sources for driving out-of-equilibrium unidirectional autocatalysis in open systems. Conclusions are drawn in Sec VI. Details of the calculation of the probability distribution for the enantiomeric excess and a stability analysis are relegated to the Appendices.

III. KINETIC MODEL

The model of Ref. [14] depicts enantiomers D or L forming from substrate A, as in Equation (1) for the reaction autocatalyzed by D (or L) and in Equation (2) for the reaction for the uncatalyzed reactions. These authors modified the original Frank model [9] in three important ways: i) the uncatalyzed background reaction is allowed to proceed in both forward and backward directions, while the Frank model considered essentially irreversible versions of the reactions in equations (1) and (2); ii) no direct reaction between D and L (termed "inhibition" in the Frank model) is included in the model; and iii) the computations in Ref. [14] are carried out in a closed system, meaning that the total number of molecules (comprising the sum of A, D, and L) remains constant over time.

$$A + D \xrightarrow{k_a} 2D \qquad A + L \xrightarrow{k_a} 2L, \tag{1}$$

$$A \underset{k_d}{\overset{k_n}{\rightleftharpoons}} D \qquad A \underset{k_d}{\overset{k_n}{\rightleftharpoons}} L. \tag{2}$$

Values for the constants were chosen in Ref. [14] as $k_a = k_n = k_d = 1$ (with appropriate

units, not given) for simulations shown in Figures 2 and 3 of Ref. [14]; the simulation shown in Figure 4 of that work set $k_n = 0$.

Equation (2) is written as a reversible reaction, which, critically, sets the theoretical equilibrium position as the ratio of the forward and backwards rate constants, k_n and k_d. The equilibrium constant, K_{eq}, is given by Equation (3):

$$K_{eq} = \frac{k_n}{k_d} = \frac{[D]_{eq}}{[A]_{eq}} = \frac{[L]_{eq}}{[A]_{eq}}. \tag{3}$$

The reactants and products in Equation (2) using $k_n = k_d = 1$ exhibit equal stability, as shown by the Gibbs free energy, $\Delta G^0 = 0$:

$$-\frac{\Delta G^0}{RT} = \ln\left(K_{eq}\right) = \ln\left(\frac{k_n}{k_d}\right) = \ln\left(\frac{1}{1}\right) = 0. \tag{4}$$

Because a catalyst can change the kinetics but not the thermodynamics of a reaction, a catalytic reaction possesses the same ΔG^0 as its uncatalyzed version. Thus Equations (3) and (4) apply equally to the reactions in Equation (1) and (2). Once the values for the three rate constants shown in Equations (1) and (2) are set, the fourth - the missing rate constant describing the reverse of Equation (1) - is fixed. The value of this rate constant, denoted k_{-a} is given by Equation (5):

$$k_{-a} = k_a \frac{k_d}{k_n}. \tag{5}$$

Equation (5) shows that, given the values chosen for the other three rate constants, k_{-a} cannot be set equal to zero. This choice would yield the nonsensical energy diagram shown in Figure 2, where the uncatalyzed reaction is allowed to proceed in both forward and reverse directions, while the catalyzed reaction experiences an infinite barrier in the reverse direction. Further, the simulation shown in Figure 4 of Ref. [14], which sets both k_{-a} and $k_n = 0$, is also thermodynamically invalid as it requires either k_a or k_d to be infinite.

A critical point that must be emphasized is that Equations (3) and (5) hold for the reaction systems of *both* Eqs. (1) and (2) regardless of whether the system is near to or far from equilibrium, or whether the system is in a transient state or exhibits a stationary non-equilibrium steady-state. Equations (3) and (5) hold equally for systems where the reverse reaction is facile as for reactions where it is virtually negligible. These equations are not dependent on the principle of microscopic reversibility or on whether detailed balance is maintained under operating conditions. (Indeed, it should be noted that any reaction system violates microscopic reversibility under productive conditions). However, even for systems

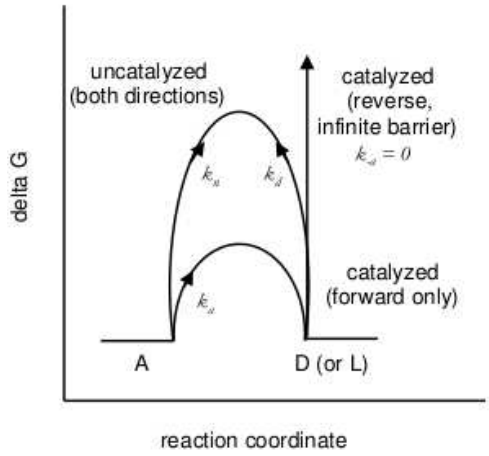

FIG. 2. Energy diagram for the catalyzed reaction of Equation (1) and the uncatalyzed reaction of Equation (2) in this work, depicted with values assigned by the work in Ref. [14].

with little prospect of ever attaining equilibrium, the relationships ordained by chemical thermodynamics dictate what is thermodynamically possible for the system. Eqs. (3) and (5) tell us that one of the rate constants cannot arbitrarily be chosen to equal zero when that choice forces another rate constant to become infinite.

The original Frank model implicitly applied an open system but did not invoke reversibility as in Equation (2), instead assuming effective irreversibility in both the autocatalytic and uncatalyzed reactions, with the latter being significantly slower. From these assumptions it follows that that k_{-a} as well as k_n and k_d have such small values (compared to k_a) that all three may be neglected. That model included a "quench" reaction removing L and D from the system, as in Equation (6), forming a product Q instead of replenishing reactant A [22].

$$D + L \xrightarrow{k_Q} Q. \tag{6}$$

Because the equilibrium position of this reaction is assumed to lie far to the right, and because this reaction is independent of Equation (1) or (2), the reverse reaction for Equation (6) may be neglected.

Goldenfeld and coworkers [14] explain in a footnote that the autocatalytic reaction of Eq. (1) is driven by an external source of energy that maintains the steady state of the system far from equilibrium, but they do not describe the source of this energy. Crucially, it must be explicitly stated that such an energy source be *chemical* in nature, in order that the equilibrium position of the autocatalytic reaction be uncoupled from that of the uncatalyzed

reaction. Any source of energy that does not yield an overall reaction stoichiometry for the autocatalyzed reaction that is different from the uncatalyzed reaction will leave the system subject to the thermodynamic constraints outlined in Equation (5), even under conditions of a far-from equilibrium steady state. This point is essential to be included in any computational model to ensure that the reaction system under study is a practically viable one that obeys the laws of chemical thermodynamics, even if that equilibrium is never attained.

The scheme in Fig 3 shows several scenarios for incorporating an independent chemical energy source into the simple Frank model in the form of reaction partners X and Y. In Case A and Case A*, the chemical quantities X and Y cross the system boundaries to undergo the autocatalytic reaction and are not accounted for in the system mass balance; these systems are open, with the reactions being irreversible in the former and reversible in the latter. In Case B, X and Y reside within the system and are included in the system mass balance: this is an isolated system. In all three cases, the total number of molecules within the system boundaries remains constant as reactions occur.

The irreversible autocatalytic reaction ($k_{-a} = 0$) and a reversible background reaction of Case A corresponds mathematically to the model of Ref. [14] if the quantity $k_a[X]$ is substituted for the rate constant k_a in that work. Modifications required to render the model in Ref. [14] chemically and thermodynamically legitimate are: i) the system is not closed to mass but is open to the passage of X and Y across the system boundaries; ii) a limitless supply of X exists external to the system, and a limitless buildup of Y is permitted external to the system; and iii) X does not react with A in the uncatalyzed reactions to form D and L. Potential scenarios for Case A could include phase boundaries as the system boundaries; for example, gaseous component X reacting with liquid phase A and D or A and L to form gaseous Y and liquid phase D or L.

Case A* generalizes Case A by allowing the autocatalytic reaction aided by reaction partners X,Y to be reversible. The reaction is reversible but it is not necessarily in equilibrium.

Case B allows the autocatalytic reaction partners X,Y to remain within the system boundaries. The system remains closed to mass, which in this case equals the sum of A, D, L, X, and Y. The reverse of the autocatalytic reaction - now modified to include the chemical energy source - must be included so that the net reaction of X to form Y does not eventually deplete X, suppressing the autocatalytic reaction and forcing the system towards the

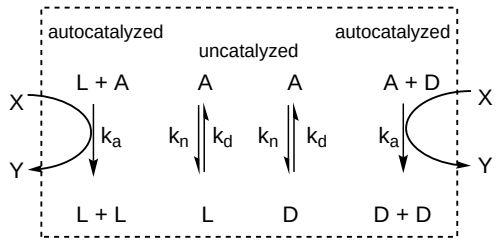

Case A: System open to mass, irreversible

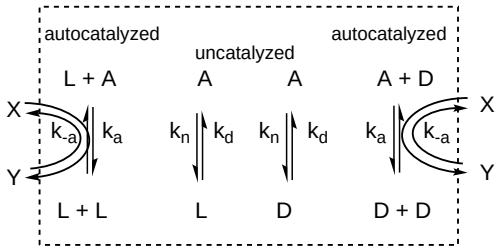

Case A*: System open to mass, reversible

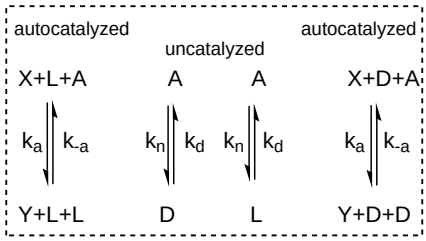

Case B: System closed to mass, reversible

FIG. 3. Independent Autocatalytic and Background Reaction Networks.

racemic state via the reversible background reaction.

The thermodynamic constraint for these autocatalytic reactions driven by external reagents is given by Eq. (7, where K'_{eq} designates the equilibrium constant for the externally driven autocatalytic reaction. It is clear that this equilibrium condition differs from that of the uncatalyzed reaction given by Eq. (3), confirming that the two reactions are independent.

$$K'_{eq} = \frac{k_a}{k_{-a}} = \frac{[L]_{eq}}{[A]_{eq}}.\frac{[Y]_{eq}}{[X]_{eq}} = \frac{[D]_{eq}}{[A]_{eq}}.\frac{[Y]_{eq}}{[X]_{eq}}. \tag{7}$$

A critical point is whether these modified scenarios are viable as models for the emergence of homochirality. This question directly addresses the generality of the model proposed in Ref. [14], namely, the conditions under which inclusion of noise suffices to stabilize the

homochiral state. Constraints on the type of feasible reactions are clearly different if the emergence of homochirality is limited to systems such as Case A, as considered in Ref. [14]. The differences between Case A, Case A*, and Case B are thus important in considering the design of possible experimental autocatalytic systems that address the origin of biological homochirality. Before examining these cases, however, we first consider the closed reaction system of Ref. [14] under fully reversible - and thus thermodynamically valid - conditions.

IV. CHIRAL AUTOCATALYSIS: NON-DRIVEN, CLOSED SYSTEM

We first consider the catalyzed and uncatalyzed reactions of Eqs. (1) and (2) including the reverse reaction of Eq. (1) with rate constant k_{-a} as described in Section II and subject to the constraints of Eqs. (3) and (5). We emphasize that, as also expressed by Wegscheider's rule [23, 24] (relating equilibrium constants with reaction rate constants and valid as well for reaction rate constant ratios for chemical cycles in non-thermodynamic states), the constraint Eq. (5) requires us to include *both* forward and reverse chemical reactions in the autocatalysis [Eq. (1)] if the uncatalyzed reaction [Eq.(2)] is assumed to be reversible. It has previously been demonstrated that this fully reversible model regarded as a deterministic system leads to the racemic state [25]; here we probe what role reaction noise might have, in order to contrast the results with those obtained when the constraint Eq. (5) is ignored as in Ref. [14].

We thus approximate the reversible scheme Eqs. (A1, 2) by means of a stochastic differential equation for the time dependence of the enantiomeric excess $\theta = ([D]-[L])/([D]+[L])$. We consider a closed well-mixed system of volume V and total number of molecules N. Taking the limit $N \gg 1$, as in [14], we arrive at the following equation for θ (see Appendix A for details):

$$\frac{d\theta}{dt} = -\frac{k_{-a}}{2+\frac{k_{-a}}{k_a}}\left(\frac{N}{V}\right)\theta + \sqrt{\frac{k_{-a}}{2V}(1-\theta^2)(2-\theta^2)}\;\eta(t), \tag{8}$$

where $\eta(t)$ is Gaussian white noise with zero mean and unit variance.

The normalized stationary distribution of Eq. (8) is given by

$$P_s(\theta) = \frac{2^{1+b}\Gamma(b+\frac{1}{2})}{\sqrt{\pi}\Gamma(b)F(\frac{1}{2},1+b,\frac{1}{2}+b;\frac{1}{2})}\,\frac{(1-\theta^2)^{b-1}}{(2-\theta^2)^{b+1}}, \qquad \text{with} \qquad b = \frac{N}{1+\frac{k_{-a}}{2k_a}}. \tag{9}$$

We plot $P_s(\theta)$ for various values of b in Fig 4. The distribution $P_s(\theta)$ is *always* peaked around the racemic state $\theta = 0$ since the parameter $b \gg 1$. As the total number of molecules N

increases, the distribution becomes ever more sharply peaked around $\theta = 0$. In particular, the probability for homochiral states $|\theta| = 1$ is strictly zero. The deterministic part of

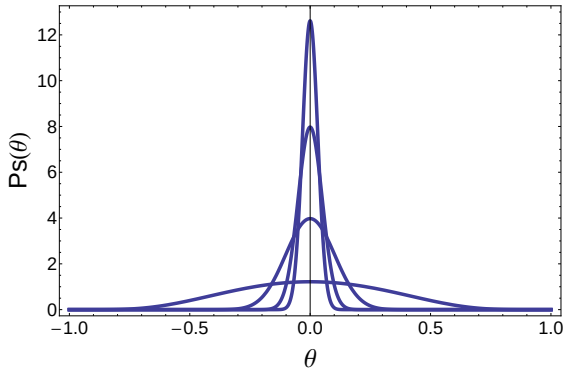

FIG. 4. Stationary probability distribution for the chiral order parameter, Eq. (9). Different values of $b = 10, 100, 400, 1000$ correspond going from the broadest to the narrowest distribution. $P_s(|\theta| = 1) = 0$ is strictly zero for homochiral states.

Eq. (8) has one fixed point at the racemic state $\theta = 0$, in accord with the stability analysis for the deterministic kinetic rate equations. The amplitude of the noise contribution is maximum for the racemic state, and vanishes at the homochiral states. Nevertheless, we cannot arrange for the noise amplitude to be greater than that of the deterministic term, as $b \gg 1$; see Eq. (9). This means that the racemic state is *stable* in the presence of reaction noise, and is surrounded by Gaussian fluctuations that become negligible for increasing total number N of molecules in the system, see Fig. 4 and Fig. 5.

To understand the stochastic dynamics, we perform simulations of the reversible scheme Eqs. (A1,2) using the Gillespie algorithm [19]. Specifically, we set $k_a = k_d = 1$ as in [14] and fix the total number of molecules to A + L + D = 1000. To illustrate the effect that stochasticity has on the dynamics, we show in Fig. 5 a short time series. It reveals that the magnitude of the fluctuations about the racemic composition depend on the rate k_n: we observe that the reaction noise is somewhat more erratic for $k_n = 0.1$ in comparison with the smoother fluctuations that result when $k_n = 10$. Note moreover the dependence of the total chiral mass proportion, defined as $([L] + [D])/([L] + [D] + [A])$: the fraction of total system mass that is chiral. Increased non-catalytic production leads to a greater proportion of chiral matter. Thermodynamics dictates $k_{-a} = 1/k_n$. This implies that smaller k_n thus leads to a greater recycling of the enantiomers back to prochiral precursor A via reverse

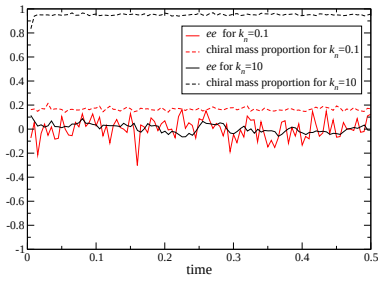

FIG. 5. Temporal series for the enantiomeric excess ee and the chiral mass proportion obtained from Gillespie simulations for different values of k_n (see inset). After a very brief transient, the curves fluctuate about the racemic state. The parameters are: $k_a = k_d = 1$ (and hence $k_{-a} = 1/k_n$), the number of molecules is 1000 (initial condition is 10 L, 10 D, 980 A). The ee is defined as $([L]-[D])/([L]+[D])$ and the chiral mass proportion as $([L]+[D])/([L]+[D]+[A])$.

autocatalysis, leading to smaller net chiral matter than when k_n is large.

The racemizing tendency of the forward rate of non-catalytic production can also be appreciated in Fig. 6 which shows the distribution in the enantiomeric excesses for different values of k_n. The greater the k_n, the more sharply peaked is the distribution about the racemic outcome, which may be seen by comparing to Fig. 4.

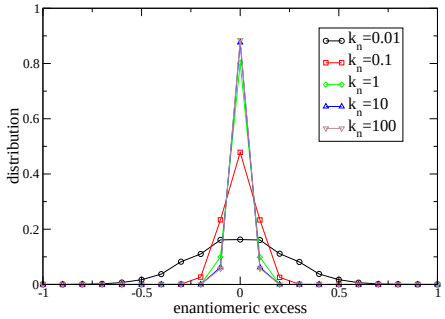

FIG. 6. Distribution of the enantiomeric excess ee obtained from Gillespie simulations for different values of k_n (see inset). After a brief initial transient, the distributions center about the racemic state. The parameters are: $V = 1$, $k_a = k_d = 1$ (and hence $k_{-a} = 1/k_n$), the number of molecules is 1000 (initial condition is 10 L, 10 D, 980 A). We obtain the $ee = ([L]-[D])/([L]+[D])$ at $T = 5$. We perform $R = 100000$ realizations. Binning is in intervals of 0.1 in the enantiomeric excess.

If the constraint Eq. (5) is overlooked and one sets $k_{-a} = 0$, then the resultant stationary

distribution is instead given by [14]

$$P(\theta) = \frac{\Gamma(\alpha + \frac{1}{2})}{\sqrt{\pi}\Gamma(\alpha)}(1-\theta^2)^{\alpha-1}, \qquad \text{with} \qquad \alpha = \frac{Vk_n}{k_a}. \tag{10}$$

This distribution can be strongly peaked at $|\theta| = 1$ if and only if $\alpha < 1$. Now consider the thermodynamic limit in which the total species population $N = A + L + D$ and the system volume V each approach infinity, while the concentration $N/V = \rho$ remains constant [19]. Then, regardless of what values are chosen for the individual rate constants k_n, k_a, the exponent $\alpha \gg 1$ will exceed unity, and the distribution function Eq.(10) will be strictly zero for $|\theta| = 1$ and strongly peaked about the racemic state $\theta = 0$, qualitatively as in Fig. 4. From this we learn that the noise induced homochiral states implied by Eq. (10) for $\alpha < 1$ are kinetic-controlled finite-size effects due to the violation of the thermodynamic constraint imposed by Eq. (5).

V. CHIRAL AUTOCATALYSIS DRIVEN BY EXTERNAL REAGENTS

As described in Section II, a bona-fide unidirectional self-replication system of the scheme given in Eqs. (1, 2) must be driven by external sources of *chemical* energy in order to maintain a non-equilibrium steady state (NESS). The steady unidirectional flow of matter in the system is a general property of steady states maintained by an energy flux [26]. To assess whether irreversible cycling can lead to a NESS with SMSB under the influence of reaction noise, we reconsider this scheme in a uniform temperature distribution driven by concentrations of reaction partners X and Y as shown in the three cases of Fig. 3.

We consider the three scenarios illustrated in Fig. 3 for incorporating independent chemical energy source. In the open systems of Cases A and A*, the chemical quantities X and Y cross the system boundary to undergo reaction and are not accounted for in the system mass balance. As mentioned in Section II, the irreversible autocatalytic reaction system of Case A corresponds to that implicitly considered in the work of Ref. [14], with k_a in that work replaced by $k_a[X]$, strictly irreversible autocatalysis with $k_{-2} = k_{-a}[Y] = 0$. For Case A*, the resultant reaction network is reversible with consumption and production of X and Y, respectively. The effective (nonzero) forward and reverse rate constants of autocatalysis are given by $k_2 = k_a[X]$, and $k_{-2} = k_{-a}[Y]$. The freedom to choose individually the two external concentrations and the rate constants arises because the thermodynamic constraint is now

given by Eq. (7) for the autocatalytic reaction while the uncatalyzed reaction continues to obey Eq. (5).

In Case B (isolated system), X and Y reside within the system, and are included in the system mass balance. In all three cases, the total number of molecules A, L, and D within the system remains constant while the reactions take place, and X and Y must be included in the stochastic Gillespie simulations. In order to avoid accumulation of X and Y molecules within the finite volume V for Cases A and A*, we define four flux terms: $\emptyset \to X$ with rate f_1, $X \to \emptyset$ with rate f_2, $\emptyset \to Y$ with rate f_3, and $Y \to \emptyset$ with rate f_4, where $\emptyset$ represents the external source/sink pool for X and Y. Gillespie simulations of the schemes for Case A, Case A* and Case B are presented jointly for comparison in Fig. 7.

A. Case A: open system; irreversible autocatalysis

The stochastic simulations of the open systems Cases A and A* require input and output flux terms to account for the external reagents that must cross the system boundaries to undergo reactions with the system molecules. In particular for Case A, where $k_{-a} = 0$, Y is not consumed by any reaction and has to be removed ($f_4 > 0$). However, since Y is not participating in any reaction, its number is irrelevant and there is no need to produce it ($f_3 = 0$). For X, we need however nonzero inflow and outflow rates $f_{1,2} \neq 0$. To be specific, we set $f_2 = f_4 = 1$ and modify the influx rate for X, f_1, for fixed k_n so that it stabilizes to a constant value.

Simulations for Case A are shown in the left hand column of Fig. (7), where we set $k_n = 0.1$. For a relatively large $f_1 = 1420$ (top), we observe a transition to the homochiral state (X stabilizes around 400). The total chiral mass is practically unity, in other words, A is essentially zero. For $k_n = 0.1$ and $f_1 = 1020$ (center image of left-hand column) the probability distribution is broadened, but still exhibits maxima at $ee = \pm 1$. The average stationary number of X is lower now. Lowering the inflow even more to $f_1 = 820$ (bottom), shows a transition towards the racemic state. Thus, varying inflow rate for X, f_1, has a similar effect as varying e.g., the rate k_n.

B. Case A*: open system; reversible autocatalysis

By marked contrast to Case A, here we include the reverse autocatalytic transformation: $k_{-a} = 1/k_n \neq 0$. Simulations for Case A* and fixed $k_n = 1$ are shown in the center column of Fig. 7. To be specific, we consider three cases with different relative inflows for X and Y: $f_1 = 999$ (top), $f_1 = 500$ (center) or $f_1 = 1$ (bottom), and $f_3 = 1000 - f_1$ for the corresponding inflows of Y. The outflow parameters for both X and Y are $f_2 = f_4 = 1$. Note that in absence of any reaction, the asymptotic values for X and Y are f_1/f_2 and f_3/f_4, respectively.

For the parameters investigated, we find the stationary outcomes always correspond to the racemic state. In this regard, we comment below on what to expect in the thermodynamic limit (large number of molecules and large volume limits) of this case and the implications of a stability analysis.

C. Case B: isolated system; reversible autocatalysis

In Case B, we fix the total numbers of X and Y to be $X + Y = 1000$ and do not require any inflow or outflow terms. In the right hand column of Fig. 7 we show the corresponding simulations where we vary k_n. X and Y are usually quite balanced, with slightly more X for low k_n ($X > 500$) and slightly more Y for high k_n ($Y > 500$). The racemic outcome is the result for the range of parameters explored.

A linear stability analysis for the equations of the reaction systems Case A, A* of Fig. 3 indicates the stable states to be expected in the thermodynamic limit for both the open Cases A and A*. As pointed out above, the external reactants impose the thermodynamic constraint of Eq. (7) for the autocatalytic reaction instead of Eq. (5) [27]. The driven, far-from-equilibrium, reaction model depends on the two independent parameters u and g:

$$u = \frac{k_d}{k_n}, \qquad g = \frac{k_{-a}[Y]}{k_a[X]}, \tag{11}$$

and the constant concentration $[C] = [L] + [D] + [A]$. The constancy in $[X], [Y]$ permits an exact analytically tractable analysis. We find that the racemic state is the unique stable outcome, and for all $u, g, [C] > 0$ (for a proof, see Appendix B). Most importantly, this indicates that the homochiral outcomes implied by the distributions for the enantiomeric excesses for the stochastic simulations of Case A, for sufficiently large influxes f_1 of X, are

the consequence of both (i) kinetic control (since $k_{-a}[Y] = 0$) and (ii) finite size effects that vanish in the thermodynamic limit [19].

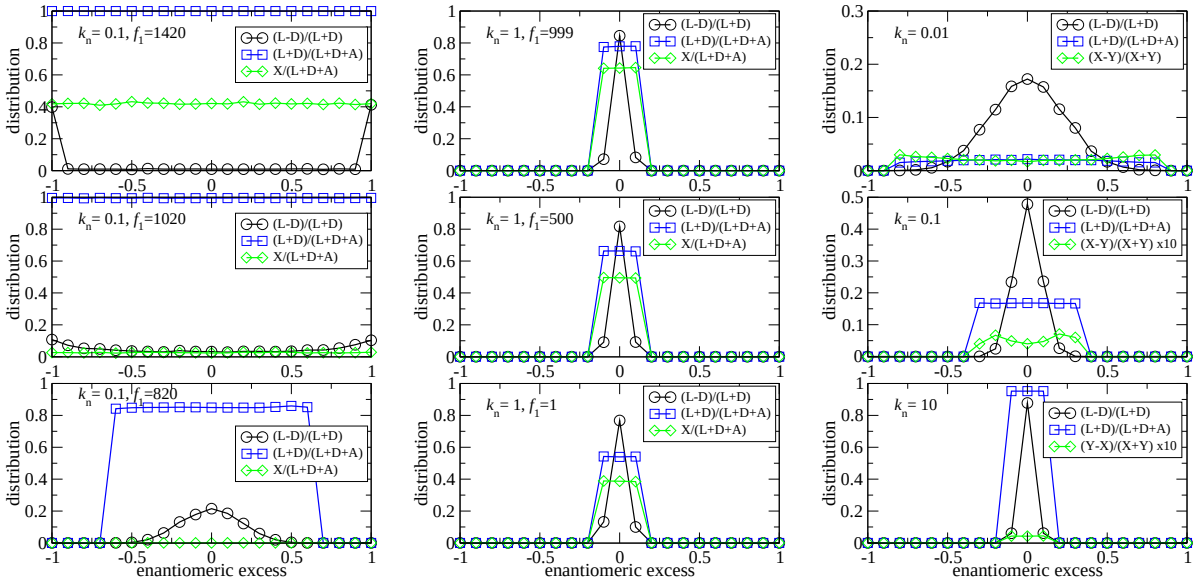

FIG. 7. Stationary distributions for the enantiomeric excess, chiral mass proportion and product bias (see insets) from Gillespie simulations of the reactions corresponding to the Cases A, A* (open) and B (isolated), in going from left to middle to right, respectively. The parameters are: $V = 1$, $k_a = k_d = 1$ (and hence $k_{-a} = 1/k_n$), for Case A* and B, whereas $k_{-a} = 0$ for Case A. The number of molecules is A+L+D=1000 (in all cases) and X+Y=1000 (Case B). See text for an explanation of the input flux f_1.

VI. CONCLUDING REMARKS

We have studied several open and isolated system scenarios of a specific autocatalytic reaction scheme subject to intrinsic reaction noise in order to assess its viability as a putative model for the emergence of homochirality. We summarize our main results below. The following points are, to some extent, inextricably interrelated.

- Thermodynamics of irreversible processes. The irreversible autocatalytic reaction of Ref. [14] was presented as a closed system. Chemical thermodynamics thus dictates that the enantioselective autocatalysis and uncatalyzed production/decay of the enantiomers must have identical ratios of the forward and reverse reaction rate constants, regardless

of whether the system is in equilibrium or far from it. Once this constraint is properly accounted for, we have demonstrated, by employing stochastic differential equations, the Fokker-Planck equation, and numerical simulations, that the resultant reaction network including reaction noise never breaks chiral symmetry. On the contrary, the unique stable outcome is always the racemic state. The homochiral states found in [14] are due to the violation of the above mentioned thermodynamic constraint.

- Driven autocatalysis. A unidirectional net flow of matter may be established in the autocatalytic reactions by coupling them to external reagents. In spite of this, an exact stability analysis, valid for the macroscopic deterministic limit, demonstrates that the manifestly out-of-equilibrium open schemes leads inexorably to the racemic state in both Case A (strictly irreversible autocatalysis) and Case A* (reversible autocatalysis). Stochastic simulations also lead to the racemic state for Case B, in which the driving reagents reside within the system (an isolated system).

- Reaction noise. The regime where stochastic kinetics is expected to be important corresponds to the case of small volumes and small numbers N of molecules. In this regard, it is established [19] that in the thermodynamic (macroscopic) limit, the intrinsic noise terms become negligibly small and the stochastic evolution equations reduce to the conventional deterministic reaction rate equations, thus establishing deterministic chemical kinetics as a limit of the former. Stochastic simulations of Case A indicate that homochirality can emerge for certain parameter choices, but the stability analysis carried out for the deterministic rate equations (*macroscopic limit*) show that the racemic solution is the unique stable outcome. These symmetry breaking results simulated in Case A are thus due to finite size, small population effects as well as kinetic control.

In summary, the effect of reaction noise and stochastic dynamics in first order autocatalytic systems such as those described in Ref. [14] and in Fig. 3 of this work, when not coupled to a mutual heterochiral interaction reaction between enantiomers, as in the case of Frank-like systems [9, 28, 29] and LES models [5, 6], most likely cannot play a role in spontaneous mirror symmetry breaking and the abiotic emergence of chirality.

ACKNOWLEDGMENTS

The research of MS, JMR and DH is supported in part by the Coordinated Project CTQ2013-47401-C2-1/2-P (MINECO). MS, JMR and DH form part of the COST Action CM1304 "Emergence and Evolution of Complex Chemical Systems". DGB acknowledges research funding from the Simons Foundation Simons Collaboration on the Origins of Life (SCOL Award 287625).

Appendix A: Probability distribution for the enantiomeric excess θ

We cast the fully reversible kinetic scheme defined by

$$A + D \underset{k_{-a}}{\overset{k_a}{\rightleftharpoons}} 2D \qquad A + L \underset{k_{-a}}{\overset{k_a}{\rightleftharpoons}} 2L, \tag{A1}$$

$$A \underset{k_d}{\overset{k_n}{\rightleftharpoons}} D \qquad A \underset{k_d}{\overset{k_n}{\rightleftharpoons}} L. \tag{A2}$$

in terms of stochastic differential equations to quantify the role played by internal reaction noise. The mapping of chemical reactions to master equations and then on to Fokker-Planck (FP) equations is an established technique [30, 31], as is the correspondence of FP with stochastic differential equations. Defining the state vector $\vec{x} = (x_1, x_2, x_3) \equiv (a, d, l)$ where a, d, l denote the time-dependent concentrations of molecules A,D and L, respectively, we find that this scheme may be approximated by the stochastic differential equation (defined in the Ito sense) [32]:

$$\frac{d\vec{x}}{dt} = \vec{H}(\vec{x}) + \boldsymbol{G}(\vec{x})\vec{\eta}(t), \tag{A3}$$

where

$$\vec{H} = \begin{pmatrix} k_{-a}(d^2 + l^2) - a(2k_n + k_a(d + l)) + k_d(d + l) \\ -k_{-a}d^2 + a(k_n + k_a d) - k_d d \\ -k_{-a}l^2 + a(k_n + k_a l) - k_d l \end{pmatrix}, \tag{A4}$$

$$\boldsymbol{G} = \frac{1}{\sqrt{V}} \begin{pmatrix} \sqrt{k_{-a}d^2 + a(k_a d + k_n) + k_d d} & \sqrt{k_{-a}l^2 + a(k_a l + k_n) + k_d l} \\ -\sqrt{k_{-a}d^2 + a(k_a d + k_n) + k_d d} & 0 \\ 0 & -\sqrt{k_{-a}l^2 + a(k_a l + k_n) + k_d l} \end{pmatrix}, \tag{A5}$$

and the η_j $(j = 1, 2)$ are Gaussian white noises with zero mean and correlation, $< \eta_i(t)\eta_j(t') >= \delta_{ij}\delta(t - t')$. V is the system volume. The rate of inverse autocatalysis is

not an independent variable, but obeys the constraint:

$$k_{-a} = k_a \frac{k_d}{k_n}. \tag{A6}$$

The number of chemical degrees of freedom $\vec{x}$ can be effectively reduced from three to one [32]. This is so because firstly, the total number of molecules is conserved by our reaction scheme, hence so is the total concentration $n = a + d + l$. Secondly, the total chiral matter $\chi = d + l$ is a *fast degree of freedom* relative to the enantiomeric excess θ [33]. Simulations of the fully reversible scheme Eqs. (A1,A2) using the Gillespie algorithm [19] confirm that χ approaches a stable fixed point value surrounded by small Gaussian fluctuations (see Fig 5). We therefore substitute $\chi(t) \to \chi^*$ into the equation for $\theta(t)$ derived below. We thus carry out the change of variables on Eq.(A3):

$$(a, d, l) \to (n, \chi, \theta) = (a + d + l, d + l, (d - l)/(d + l)), \tag{A7}$$

employing Ito's formula [30]:

$$df(\vec{x}) = [\sum_i H_i(\vec{x})\partial_i f(\vec{x}) + \frac{1}{2}\sum_{i,j}[\boldsymbol{G}\boldsymbol{G}^T]_{ij}\partial_i\partial_j f(\vec{x})]dt + \sum_{ij}\boldsymbol{G}(\vec{x})_{ij}\partial_i f(\vec{x})dW_j(t). \tag{A8}$$

From Eq. (A8) it is straightforward to demonstrate that $\frac{dn}{dt} \equiv 0$ is identically zero, as it must be. From $\frac{d\chi}{dt} = 0$ we solve for the fixed point χ^*:

$$\chi^*(\bar{\theta}) = \frac{k_a n - 2k_n - k_d + \sqrt{(k_a n - 2k_n - k_d)^2 + 8nk_n[k_a + \frac{1}{2}(1 + \bar{\theta}^2)k_{-a}]}}{2k_a + (1 + \bar{\theta}^2)k_{-a}}, \tag{A9}$$

Since $\chi \geq 0$, we take the positive root. Note the total chiral matter $\chi^*(\bar{\theta})$ depends *weakly* on the most probable stationary value $0 \leq \bar{\theta}^2 \leq 1$ for the chiral order parameter. The most probable value of $\bar{\theta}$ is determined from the stochastic differential equation for $\theta(t)$. We prove below that *self-consistency* requires taking $\bar{\theta} = 0$ in Eq. (A9).

We derive the stochastic equation obeyed by $\theta(t)$ and substitute $\chi^*(0)$ into this equation. We express the result in terms of the total number of molecules $N = Vn$ and for $N \gg 1$. The enantiomeric excess or chiral order parameter θ obeys the equation

$$\frac{d\theta}{dt} = -\frac{k_{-a}}{2 + \frac{k_{-a}}{k_a}}(\frac{N}{V})\theta + \sqrt{\frac{k_{-a}}{2V}(1 - \theta^2)(2 - \theta^2)}\ \eta(t), \tag{A10}$$

where $\eta(t)$ is Gaussian white noise with zero mean and unit variance.

From the Fokker-Planck equation corresponding to Eq. (A10) we readily solve for the steady state probability distribution $P_s(\theta)$ for θ [31]. We find:

$$P_s(\theta) = \mathcal{N}\frac{(1-\theta^2)^{b-1}}{(2-\theta^2)^{b+1}}, \qquad \text{with} \qquad b = \frac{N}{1+\frac{k_{-a}}{2k_a}}, \tag{A11}$$

and the normalization constant

$$\mathcal{N} = \Big(\int_{-1}^{1} d\theta\, \frac{(1-\theta^2)^{b-1}}{(2-\theta^2)^{b+1}}\Big)^{-1} = \frac{2^{1+b}\Gamma(b+\frac{1}{2})}{\sqrt{\pi}\Gamma(b)F(\frac{1}{2},1+b,\frac{1}{2}+b;\frac{1}{2})}, \tag{A12}$$

where F is the hypergeometric function [34].

From P_s we conclude (see Fig 4) that the most probable value for the chiral order parameter is $\bar{\theta} = 0$, corresponding to the racemic state, thus establishing the self-consistency of employing this value in Eq. (A9).

Appendix B: Stability analysis for externally driven autocatalysis

We express the kinetic rate equations for the driven autocatalysis

$$A + L + X \underset{k_{-a}}{\overset{k_a}{\rightleftharpoons}} L + L + Y, \qquad A + D + X \underset{k_{-a}}{\overset{k_a}{\rightleftharpoons}} D + D + Y, \tag{B1}$$

$$A \underset{k_d}{\overset{k_n}{\rightleftharpoons}} L, \qquad A \underset{k_d}{\overset{k_n}{\rightleftharpoons}} D. \tag{B2}$$

in terms of dimensionless rates and concentrations [6, 35]. Changing variables to $\chi = L + D, y = L - D$, we find

$$\frac{d\chi}{d\tau} = 2A + (A-u)\chi - \frac{g}{2}(\chi^2 + y^2), \tag{B3}$$

$$\frac{dy}{d\tau} = y(A - u - g\chi), \tag{B4}$$

where $\tau = k_n t$ is dimensionless time, $(C, A, \chi, y) = \frac{k_a}{k_n}([C], [A], [\chi], [y])$ the dimensionless concentrations, and

$$A = C - \chi, \qquad u = \frac{k_d}{k_n}, \qquad g = \frac{[Y]k_{-a}}{[X]k_a}. \tag{B5}$$

Eqs. (B3,B4) admit a stationary racemic and two mirror symmetric chiral solutions:

$$y = 0, \qquad \chi = \frac{C - 2 - u + \sqrt{C^2 + C(4+4g-2u) + (2+u)^2}}{2+g}, \tag{B6}$$

$$y = \pm\frac{\sqrt{C^2 g + 2Cg(2+2g-u) + u(4+g(4+u))}}{\sqrt{g(1+g)^2}}, \qquad \chi = \frac{C-u}{1+g}. \tag{B7}$$

To assess dynamic stability, we linearize the equations Eqs.(B3,B4) in arbitrary fluctuations $\delta\chi, \delta y$ about the stationary solutions. Their time dependence is determined by

$$\frac{d}{d\tau}\begin{pmatrix}\delta y\\ \delta\chi\end{pmatrix} = \boldsymbol{A}\begin{pmatrix}\delta y\\ \delta\chi\end{pmatrix}, \tag{B8}$$

where

$$\boldsymbol{A} = \begin{pmatrix} A-u-g\chi & -(g+1)y \\ -gy & A-2-u-(g+1)\chi \end{pmatrix}. \tag{B9}$$

We evaluate $\boldsymbol{A}$ over the stationary solutions Eqs. (B6,B7) and calculate the corresponding pair (λ_1, λ_2) of eigenvalues. We find that:

$$\lambda_1 < 0 \;\&\; \lambda_2 < 0, \qquad \forall\, C > 0, g > 0, u > 0, \qquad (\textbf{racemic}) \tag{B10}$$

whereas for both the chiral solutions

$$\lambda_1 < 0 \;\&\; \lambda_2 > 0, \qquad \forall\, C > 0, g > 0, u > 0, \qquad (\textbf{chiral}). \tag{B11}$$

This establishes that externally driven autocatalysis Eq. (B1) together with noncatalytic production Eq. (B2) yields the racemic solution as the unique final stable state.

---

[1] P. Cintas (Editor), *Biochirality: Origins, Evolution and Molecular Recognition* (Springer-Verlag, Heidelberg, 2013).

[2] Systems capable of SMSB yield large net chiral excesses, mostly in the vicinity of homochirality, as common non-thermodynamic states [3]. In closed systems with relatively high exergonic transformations, prolonged chiral excursions i.e., kinetically controlled chiral outcomes, are possible [4]. Final stationary chiral states are possible in either open or in closed systems prevented from coming into thermodynamic equilibrium with their surroundings; see, for example, Refs. [5, 6]

[3] J.M. Ribó, C. Blanco, J. Crusats, Z. El-Hachemi, D. Hochberg and A. Moyano, Absolute Asymmetric Synthesis in Enantioselective Autocatalytic Reaction Networks, Chem. Eur. J. **20**, 17250 (2014).

[4] J. Crusats, D. Hochberg, A. Moyano and J.M. Ribó, Frank Model and Spontaneous Emergence of Chirality in Closed Systems, ChemPhysChem **10** (12), 2123 (2009).

[5] C. Blanco, J.M Ribó, J. Crusats, Z. El-Hachemi, A. Moyano and D. Hochberg, Mirror symmetry breaking with limited enantioselective autocatalysis and temperature gradients, Phys. Chem. Chem. Phys. **15**, 1546 (2013).

[6] C. Blanco, J. Crusats, Z. El-Hachemi, A. Moyano, D. Hochberg and J.M. Ribó, Spontaneous Emergence of Chirality in the Limited Enantioselective Model: Autocatalytic Cycle Driven by an External Reagent, ChemPhysChem **14**, 2432-2440 (2013).

[7] A. Guijarro and M. Yus, *The Origin of Chirality in the Molecules of Life* (RSC Publishing, Cambridge, 2009)

[8] V. Avetisov and V. Goldanskii, Mirror symmetry breaking at the molecular level, Proc. Natl. Acad. Sci. USA **93**, 11435 (1996).

[9] F. C. Frank, On spontaneous asymmetric synthesis. Biochim. Biophys. Acta **11**, 459-463 (1953).

[10] K. Soai, T. Shibata, H. Morioka, and K. Choji, Asymmetric Autocatalysis And Amplification Of Enantiomeric Excess Of A Chiral Molecule, Nature (London) **378**, 767 (1995).

[11] D. G. Blackmond, Asymmetric Autocatalysis and its Implications for the Origin of Homochirality, Proc. Natl. Acad. Sci. USA, **101**, 5732 (2004).

[12] D.G. Blackmond, "If pigs could fly" chemistry: a tutorial on the principle of microscopic reversibility, Angew. Chemie. Int. Ed., **48** 2648 (2009).

[13] J.M. Ribó and D. Hochberg, Competitive Exclusion Principle in Ecology and Absolute Asymmetric Synthesis in Chemistry, Chirality **27**, 722-727 (2015).

[14] F. Jafarpour, T. Biancalani, N. Goldenfeld, Noise-Induced Mechanism for Biological Homochirality of Early Life Self-Replicators, Phys. Rev. Lett. **115**, 158101 (2015).

[15] D. G. Blackmond, The Origin of Biological Homochirality, in *The Origin of Life*, ed. no.; Deamer, D.; Szostak, J.W., Cold Spring Harbor Laboratory Press, 2010.

[16] W.H. Mills, Some Aspects of Stereochemistry, Chem. Ind. (London) **51**, 750-759 (1932).

[17] K. Mislow, Absolute Asymmetric Synthesis: A Commentary, Collect. Czech. Chem. Commun. **68**, 849-864 (2003).

[18] N.G. van Kampen, *Stochastic Processes in Physics and Chemistry* (Elsevier, Amsterdam, 2007).

[19] D. T. Gillespie, Stochastic Simulation of Chemical Kinetics, Annu. Rev. Phys. Chem. **58**, 35-55 (2007).

[20] J. Puchalka, A. M. Kierzek, Bridging the gap between stochastic and deterministic regimes in the kinetic simulations of the biochemical reaction networks, Biophys. J. **86**, 1357-72 (2004)

[21] P. Erdí and G. Lente, *Stochastic Chemical Kinetics: Theory and (Mostly) Systems Biological Applications*. (Springer Series in Synergetics, Springer, New York, 2014).

[22] Values for the constants in the introductory simulations in Figure 1 of Ref [14] are not given. The first paragraph of the text and Fig. 1a in Ref [14] incorrectly attributes the reaction $D + L \rightarrow 2A$ to Frank's model (see explanation in Footnote [4] of that work).

[23] R. Wegscheider, Über simultane Gleichgewichte und die Beziehung zwischen Thermodynamic und Reaktionskinetic homogener Systeme, Monatsh Chem **32** 849-906 (1901).

[24] A.N. Gorban and G.S. Yablonsky, Extended detailed balance for systems with irreversible reactions, Chem. Eng. Sci. **66**, 5388 (2011).

[25] D.G. Blackmond and O.K. Matar, Re-Examination of Reversibility in Reaction Models for the Spontaneous Emergence of Homochirality, J. Phys. Chem. B **112**, 5098-5104 (2008).

[26] L. Onsager, Reciprocal Relations in Irreversible Processes I, Phys. Rev. **37**, 405 (1931); Reciprocal Relations in Irreversible Processes II, Phys. Rev. **38**, 2265 (1931).

[27] For driven catalysis, the external reagents lead to two independent dimensionless variables g, u, compared to one variable in the undriven case.

[28] D. G. Blackmond, C. R. McMillan, S. Ramdeehul, A. Schorm, J. M. Brown, Origins of Asymmetric Amplification in Autocatalytic Alkylzinc Additions, J. Am. Chem. Soc. 2001, 123, 10103-10104.

[29] R. Plasson, D. K. Kondepudi, H. Bersini, A. Commeyras, K. Asakura, Emergence of homochirality in far-from-equilibrium systems: Mechanisms and role in prebiotic chemistry. Chirality **19**, 589-600, (2007)

[30] C.W. Gardiner, *Handbook of Stochastic Methods for Physics, Chemistry and the Natural Sciences* 2nd ed. (Springer-Verlag, Berlin, 1997).

[31] H. Risken, *The Fokker-Planck Equation, Methods of Solution and Applications* 2nd ed. (Springer, Berlin, 1989).

[32] See, http://link.aps.org/supplemental/10.1103/PhysRevLett.115.158101 and the references therein.

[33] D. Hochberg and M-P. Zorzano, Mirror symmetry breaking as a problem in dynamic critical phenomena, Phys. Rev. E **76**, 0211109 (2007).

[34] H. Hochstadt, *The Functions of Mathematical Physics* (Dover, New York, 1986), Chap. 4.

[35] J.M. Ribó and D. Hochberg, Stability of racemic and chiral steady states in open and closed chemical systems, Phys. Lett. **A** 373, 111-122 (2008).